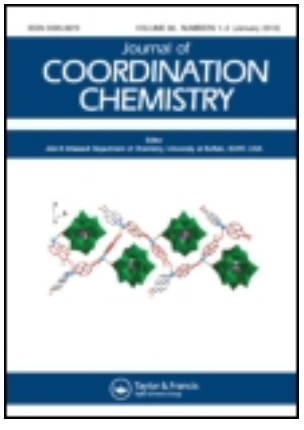

Journal of Coordination Chemistry
Publication details, including instructions for authors and subscription information:
http://www.tandfonline.com/loi/gcoo20

Structural and calorimetric investigations of a highly disordered crystal $[Co(NH_3)_6](BF_4)_3$

Natalia Górska [a c], Akira Inaba [a], Yasukazu Hirao [b] & Edward Mikuli [c]

[a] Research Center for Structural Thermodynamics, Graduate School of Science, Osaka University, Toyonaka, Japan

[b] Department of Chemistry, Graduate School of Science, Osaka University, Toyonaka, Japan

[c] Faculty of Chemistry, Department of Chemical Physics, Jagiellonian University, Kraków, Poland

Accepted author version posted online: 21 Feb 2013.Published online: 05 Apr 2013.

To cite this article: Natalia Górska, Akira Inaba, Yasukazu Hirao & Edward Mikuli (2013) Structural and calorimetric investigations of a highly disordered crystal $[Co(NH_3)_6](BF_4)_3$, Journal of Coordination Chemistry, 66:7, 1238-1251, DOI: 10.1080/00958972.2013.777834

To link to this article: http://dx.doi.org/10.1080/00958972.2013.777834

Journal of Coordination Chemistry, 2013
http://dx.doi.org/10.1080/00958972.2013.777834

Structural and calorimetric investigations of a highly disordered crystal $[Co(NH_3)_6](BF_4)_3$

NATALIA GÓRSKA*†§, AKIRA INABA†, YASUKAZU HIRAO‡ and EDWARD MIKULI§

†Research Center for Structural Thermodynamics, Graduate School of Science, Osaka University, Toyonaka, Japan
‡Department of Chemistry, Graduate School of Science, Osaka University, Toyonaka, Japan
§Faculty of Chemistry, Department of Chemical Physics, Jagiellonian University, Kraków, Poland

(*Received 21 April 2012; in final form 10 January 2013*)

Five crystalline phases of $[Co(NH_3)_6](BF_4)_3$ were identified by adiabatic calorimetry. Two phase transitions at $T_{C1}(II \rightarrow I) = 271.7\,K$ and $T_{C2}(III \rightarrow II) = 152.2\,K$ are accompanied by large entropy changes (8.4 and $6.5\,J\,K^1\,mol^1$, respectively), whereas two additional transitions at $T_{C3}(IV \rightarrow III) = 67.4\,K$ and $T_{C4}(V \rightarrow IV) = 48.9\,K$ are accompanied by small entropy changes (0.31 and $0.15\,J\,K^{-1}\,mol^{-1}$, respectively). X-ray single-crystal diffraction at 293 K demonstrates that phase I is cubic ($Z = 4$) and that two types of anions exist with different types of orientational disorder. In phase II, at 200 K, which is also a cubic system ($Z = 32$), five anions (out of 12) become ordered, and three cations (out of four) are deformed to give a lower symmetry. This is attributed to the orientational ordering of the anions triggered by NH···F hydrogen-bonding interactions. Further ordering of the anions and the symmetry reduction of the crystal occurred at T_{C2}, but the structure of phase III still remained cubic. The energies required to reorient an ordered anion in the crystal lattice of phases II and III were estimated from the excess heat capacity, demonstrating that the NH···F hydrogen-bonding interactions in this compound are considerably weaker than the NH···O interactions in an isostructural compound, $[Co(NH_3)_6](ClO_4)_3$.

Keywords: X-ray diffraction; Calorimetry; Crystal structure; Phase transition; Disordered system

1. Introduction

The hexamine complex cation with a divalent or trivalent metal (M) at the center, where the NH_3 ligands rotate nearly freely around their threefold axes, has a regular octahedral symmetry even in crystals over a wide temperature range. The solid polymorphism of coordination compounds of the $[M(NH_3)_6](XY_4)_2$ type ($XY_4^- = ClO_4^-$ or BF_4^-) has been studied extensively using various methods, such as calorimetry, X-ray diffraction, neutron scattering, NMR, and vibrational spectroscopy, as well as theoretical considerations [1–5]. These compounds crystallize in a cubic system ($Fm\bar{3}m$ space group; No. 225) at high

*Corresponding author. Email: gorska@chem.sci.osaka-u.ac.jp

temperature and transform into a monoclinic system at low temperature with considerable reduction of symmetry. Interestingly, $[M(NH_3)_6](XY_4)_3$ with a trivalent central metal also crystallize in a cubic system. However, the phase behavior at low temperature is significantly different. We previously studied the crystal structure of $[Co(NH_3)_6](ClO_4)_3$ and its phase behavior [6]. The high-temperature phase (phase I) crystallizes in the same space group similar to divalent compounds, whereas phase II still belongs to a cubic system ($Ia\bar{3}$ space group, No. 206). Both phases are highly disordered in the orientation of the ClO_4^- anions and the phase transition between them is accompanied by a large entropy change.

In this study, we investigated $[Co(NH_3)_6](BF_4)_3$. According to X-ray powder diffraction [7], the compound crystallizes in a cubic system ($Fm\bar{3}m$, $Z=4$) with lattice parameter $a=11.211$ Å at room temperature. The crystal in phase I is considered to be isostructural with four other compounds of the same type [6–10]: $[Co(NH_3)_6](ClO_4)_3$, $[Cr(NH_3)_6](BF_4)_3$, $[Cr(NH_3)_6](ClO_4)_3$, and $[Ru(NH_3)_6](BF_4)_3$. For the phase behavior, an NMR study [11] indicated a motional narrowing in the second moments of the ^1H and ^{19}F resonances between 250 and 295 K.

As described below, we precisely examined the phase behavior of $[Co(NH_3)_6](BF_4)_3$ by adiabatic calorimetry and X-ray single-crystal diffraction (XRSCD) and discuss the possible mechanism of the phase transitions.

2. Experimental

2.1. *Materials*

A few grams of $[Co(NH_3)_6](NO_3)_3$, previously prepared according to the procedure by Bjerrum and McReynolds [12], were dissolved in deionized water, and a 40% HBF_4 solution (Wako Pure Chem. Ind., Ltd.) was slowly added. The solution was then chilled, and fine orange crystals of $[Co(NH_3)_6](BF_4)_3$ were precipitated, washed with ethanol, and dried in air. Since the compound slowly decomposes in light, it was placed in a sealed vessel to protect it from light. Single crystals for XRSCD measurements were obtained at 280 K by slow evaporation from aqueous solution. The composition was determined by elemental analysis on a EURO EA 3000 instrument based on N and H content of the NH_3 ligands. Anal. Calcd (%): N, 19.94; H, 4.30. Found: N, 19.90; H, 4.15.

2.2. *Methods*

Heat capacity measurements were conducted between 5 and 300 K using a laboratory-made adiabatic calorimeter. The polycrystalline sample was placed in a gold-plated copper cell with an inner volume of 2.77 cm^3. The mass of the loaded sample was 0.65483 g (1.5535 mmol). Helium exchange gas was used to attain equilibrium within the cell. The temperature was measured by a rhodium–iron alloy resistance thermometer, whose temperature scale is based on ITS-90. The heat capacity of the empty cell was measured in advance and subtracted from the total heat capacity. More details concerning this experiment can be found in previous articles [13, 14].

The XRSCD data were collected on two different diffractometers with filtered Mo–Kα radiation. A good-quality orange crystal with dimensions $0.2 \times 0.2 \times 0.2\,mm^3$ was investigated with a Rigaku R-AXIS VII diffractometer. The crystal-to-detector distance

Table 1. Crystallographic data for $[Co(NH_3)_6](BF_4)_3$ at 293 and 200 K.

Crystallographic method	Single-crystal diffraction	Single-crystal diffraction
Diffractometer	Rigaku R-AXIS RAPID	Rigaku R-AXIS VII
Radiation	μ(MoKα) ($\lambda = 0.71075$ Å)	μ(MoKα) ($\lambda = 0.71075$ Å)
Empirical formula	$[Co(NH_3)_6](BF_4)_3$	$[Co(NH_3)_6](BF_4)_3$
Formula weight	421.56 g mol^{-1}	421.56 g mol^{-1}
Temperature	293 K	200 K
Crystal system	Cubic	Cubic
Space group	$Fm\bar{3}m$ (No. 225)	$Ia\bar{3}$ (No. 206)
Lattice parameters	$a = 11.2462(8)$ Å	$a = 22.3460(4)$ Å
Volume	1422.39(18) Å^3	11158.3(3) Å^3
Z	4	32
D_{Calcd}	1.969 g cm^{-3}	2.008 g cm^{-3}
F_{000}	840	6720
Θ range for data collection	3.14°–34.67°	3.16°–27.48°
No. of reflections measured	Total: 5027	Total: 64188
	Unique: 193 ($R_{int} = 0.0272$)	Unique: 2139 ($R_{int} = 0.0312$)
Structure solution	Direct methods	Direct methods
Refinement method	Full-matrix least-squares on F^2	Full-matrix least-squares on F^2
Reflection/parameter ratio	10.16	14.26
Goodness of fit on F^2	1.301	1.145
R indices	$R1 = 0.0639$; $wR2 = 0.1658$	$R1 = 0.1014$; $wR2 = 0.2825$

was 200.0 mm. Measurements were conducted at 100, 200, and 300 K. After these measurements, another crystal with dimensions $0.3 \times 0.3 \times 0.3$ mm^3 was also investigated at 293 K with a Rigaku R-AXIS RAPID diffractometer. The crystal-to-detector distance was 127.0 mm. All data were collected with a temperature accuracy of ±2 K. The results obtained at 300 and 293 K were consistent, and we present here the data at 293 K because it showed better refinement accuracy. A full analysis of the crystal structures at 293 and 200 K was conducted by direct methods (SHELX-97 and SIR2004) [15, 16] using Yadokari-XG 2009 [17]. Crystallographic data have been deposited at the CCDC, 12 Union Road, Cambridge CB2 1EZ, UK. The deposition number is 874058. The details of these measurements are listed in table 1.

3. Results and discussion

3.1. *Calorimetric investigations*

Figure 1 illustrates the molar heat capacity (C_p) determined by adiabatic calorimetry and the inset shows the magnified view at low temperatures. The data are listed in Supplemental material. The compound exhibits four solid–solid phase transitions, with two large anomalies at $T_{C1} = 271.7$ K (phase II → I) and $T_{C2} = 152.2$ K (III → II) and two small anomalies at $T_{C3} = 67.4$ K (IV → III) and $T_{C4} = 48.9$ K (V → IV). The thermodynamic parameters for all transitions were evaluated by estimating a "normal" heat capacity curve, as indicated in figure 1. Figure 2 shows the excess heat capacity, and the results obtained are summarized in table 2.

The II → I transition has two separate peaks with an additional peak at 267.4 K, and the III → II transition has a small hump on the low-temperature side (see figure 2). For both

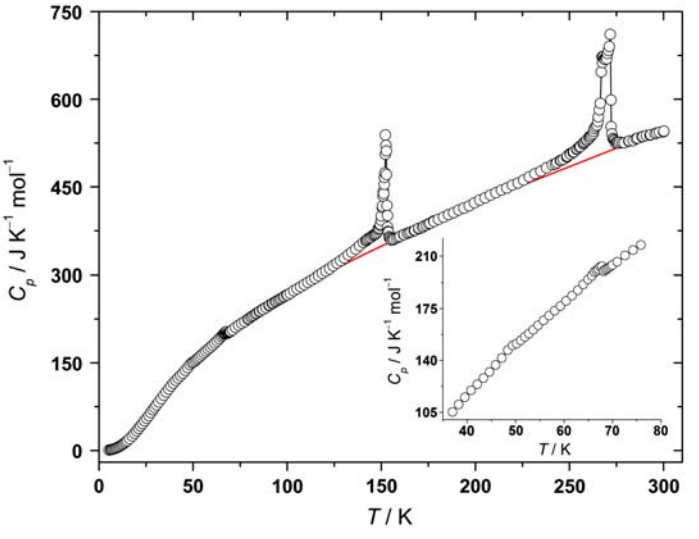

Figure 1. Molar heat capacity C_p obtained for $[Co(NH_3)_6](BF_4)_3$. The baseline for the phase transitions is shown. Inset: C_p between 35 and 80 K.

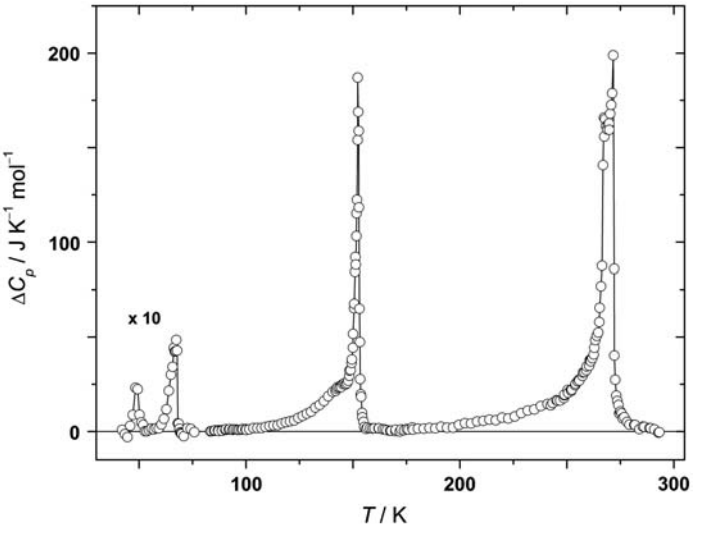

Figure 2. Excess heat capacity obtained for $[Co(NH_3)_6](BF_4)_3$. Low-temperature anomalies are magnified.

Table 2. Thermodynamic parameters of phase transitions of $[Co(NH_3)_6](BF_4)_3$.

Phase change	T (K)	ΔH (J mol^{-1})	ΔS (J K^{-1} mol^{-1})
II → I	271.7 (267.4)	2141	8.42
III → II	152.2	915	6.50
IV → III	67.4	19.7	0.31
V → IV	48.9	7.5	0.15

transitions, the low-temperature tail of the heat capacity is characteristic. It is interesting to note here that the ^{1}H and ^{19}F resonance lines show motional narrowing at T_{C1} [11], where the dynamics of both cations and anions are dramatically changed. On the other hand, no dynamical change was observed at T_{C2} in the NMR study. The total entropy change ($15.4\,J\,K^{-1}\,mol^{-1}$) is large, being comparable with that obtained for divalent compounds ($13–33\,J\,K^{-1}\,mol^{-1}$) [18–21]. This reveals that the transitions are essentially of an order–disorder type. No anomalous behavior was observed in the temperature drift during the measurements, indicating that all the phases obtained here are stable at that temperature. This is in contrast to our previous results obtained for $[Co(NH_3)_6](ClO_4)_3$, in which both stable and metastable phases are involved [6].

3.2. *Structural investigations*

3.2.1. Crystal structure of phase I. As described in table 1, the compound in phase I at 293 K crystallizes in a cubic system ($Fm\bar{3}m$, No. 225, fcc) with four formula units in the unit cell and with the lattice parameter $a = 11.2462(8)$ Å. This space group is not compatible with the threefold symmetry of NH_3 ligands, and because of their fast rotation around the Co–N axes, the hydrogens were ignored, and only the positional and thermal parameters of Co, B, F, and N atoms were refined. The atomic coordinates and isotropic displacement parameters of nonhydrogen atoms at 293 and 200 K are listed in Supplementary material and selected bond lengths and angles are listed in table 3.

Figure 3(a) shows nonequivalent units obtained in phase I. One type of coordination cation, $Co(NH_3)_6^{3+}$, having a regular octahedral symmetry with all Co–N bond distances equal to 1.968 Å and two types of BF_4^- anions of tetrahedral symmetry with different types of orientational disorder are identified. Every anion with a B1 at the [0 0 ½] position in the unit cell, hereafter designated as "cubic," is surrounded by eight half F atoms placed symmetrically at the vertices of a regular cube with all B1–F1 distances equal to 1.406 Å. This type of disorder is often observed for tetrahedral anions and is the result of a 90° rotation of the anion around any of its fourfold axes enabling its interconversion between two nonequivalent positions, which correspond to two possible orientations. There are four cubic anions (out of 12) in the unit cell of phase I.

We now turn to anions with B2 at the [¼ ¼ ¼] position [see figure 3(a)]. Every anion of this type is disordered in such a way that six partial F2 are placed at the vertices of a regular octahedron with all B2–F2 bond distances equal to 1.461 Å, and the next four partial F3 are placed at the vertices of a regular tetrahedron with B2–F3 bond distances shorter than or equal to 1.273 Å. It is difficult to say exactly how many possible orientations can be distinguished in this case, but this type of anion may have more freedom to form different orientations. The anion is placed at a much longer distance from the NH_3 ligands than the cubic anion (the closest N–B1 and N–B2 distances are 3.655 and 4.065 Å, respectively). This type of disordered anion has an adamantane-like geometry, hereafter designated as an "adamantane" anion.

Figure 4(a) shows the anionic pattern in the unit cell of phase I. The cubic anions are located at the center of the unit cell and at the middle of the edges. The adamantane anions fill up the channels formed between cubic anions. This compound in phase I is isostructural with $[Co(NH_3)_6](ClO_4)_3$ in phase I [6]. The type of orientational disorder of the anions is exactly the same between the two crystals.

Table 3. Selected interatomic distances (Å) and angles (°) of $[Co(NH_3)_6](BF_4)_3$ at 293 and 200 K.

293 K		200 K	
Distances (Å)			
Co1–N1	1.968(4)	Co1–N1	1.966(5)
		Co2–N2	1.966(6)
		Co2–N3	1.970(6)
		Co2–N4	1.969(4)
		Co2–N5	1.973(4)
N1–B1	3.655	N1–B1	3.618
		N1–B2	3.623
		N1–B3	4.108
N1–B2	4.065	N1–B4	4.030
		N2–B2	3.591
		N2–B4	4.098
		N3–B2	3.647
		N3–B3	4.066
		N4–B3	4.141
		N4–B4	3.936
		N5–B3	4.103
		N5–B4	3.903
N1–F1	3.066	N2–F3(B2)	2.973
N1–F2	3.231	N3–F5(B3)	2.863
N1–F3	2.940	N5–F1(B1)	3.062
		N5–F2(B1)	2.904
B1–F1	1.406(8)	B1–F1	1.357(6)
		B1–F2	1.519(12)
B2–F2	1.461(8)	B2–F3	1.417(7)
B2–F3	1.273(13)	B2–F4	1.374(7)
		B3–F5	1.368(5)
		B3–F6	1.414(13)
		B1–B3	4.753
B1–B2	4.870	B1–B4	4.852
		B3–B4	5.563
Angles (°)			
N1–Co1–N1	90	N1–Co1–N1	90.28(19)
N1–Co1–N1′	180	N1–Co1–N1′	89.72(19)
		N5–Co2–N2	90.29(13)
		N5–Co2–N3	89.71(13)
F1–B1–F1	70.529(2)	F1–B1–F1	66.8(2)
F1–B1–F1′	109.471(2)	F1–B1–F1′	113.2(2)
		F1–B1–F2	105.4(3)
		F3–B2–F3	106.7(7)
		F4–B2–F4	112.4(8)
		F5–B3–F5	111.1(5)
		F5–B3–F6	107.7(5)

Description of symbols at 293 K: B1: derived from cubic-type disordered BF_4^-;
B2: adamantane-type disordered BF_4^-.
Description of symbols at 200 K: B1: derived from of cubic-type disordered BF_4^-;
B2: ordered BF_4^- (from cubic type); B3: ordered BF_4^- (from adamantane type);
B4: adamantane-type disordered BF_4^-.

3.2.2. Crystal structure of phase II. The compound in phase II at 200 K crystallizes in the cubic space group $Ia\bar{3}$ (No. 206), with 32 formula units in the unit cell and with the double lattice parameter $a = 22.3460(4)$ Å in comparison with the result obtained in phase I at 293 K (11.2462 Å). The crystal structure could be determined assuming that the rotation of hydrogens around the Co–N axes is still rapid. Figure 3(b) illustrates the nonequivalent units in phase II with two types of $Co(NH_3)_6^{3+}$ cations. One type essentially has a regular

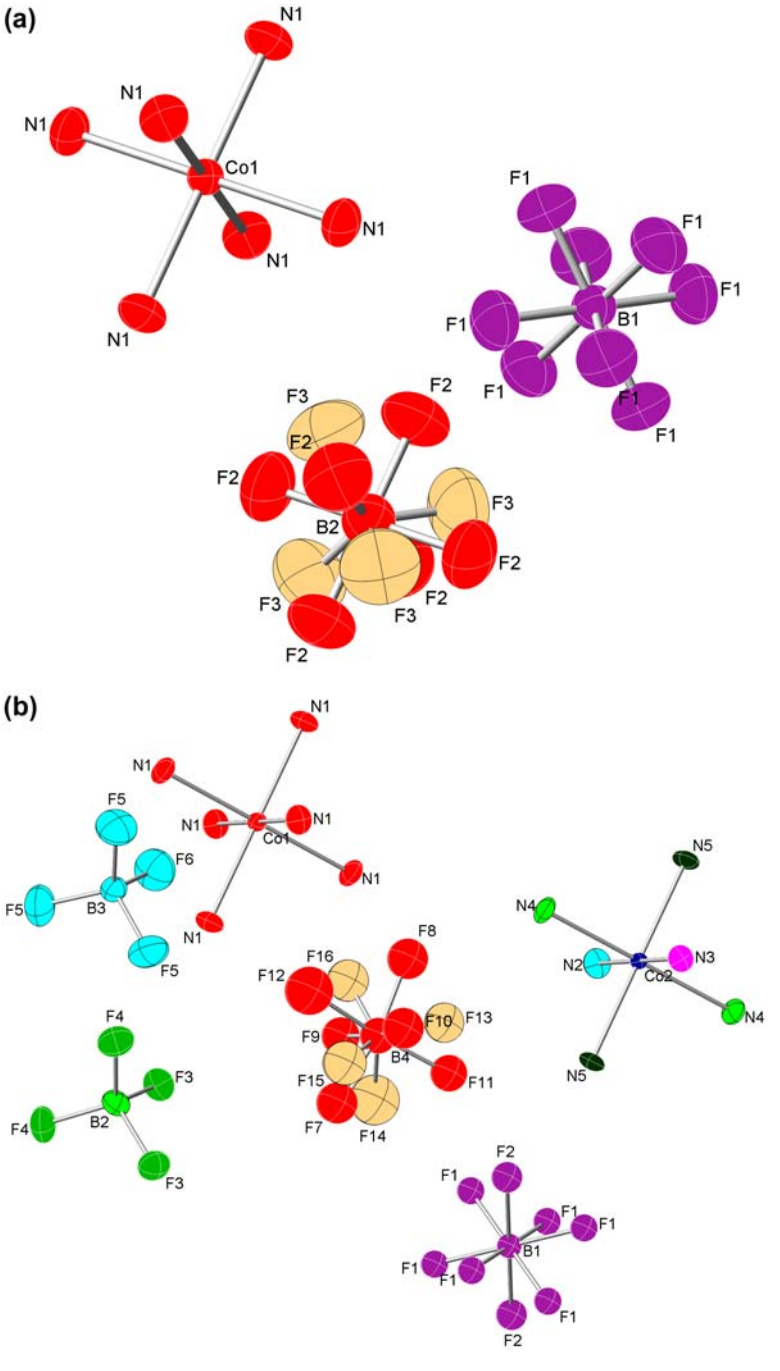

Figure 3. Structural units of $[Co(NH_3)_6](BF_4)_3$ showing the atom-numbering scheme at 293 K (a) and 200 K (b). Displacement ellipsoids are drawn at the 50% probability level.

octahedral geometry with all Co–N bond distances equal to 1.966 Å and with the N–Co–N angles slightly distorted (89.72° and 90.28°). The other type of cation is clearly deformed with two pairs of Co–N bonds equal to 1.969 and 1.973 Å. The remaining two Co–N

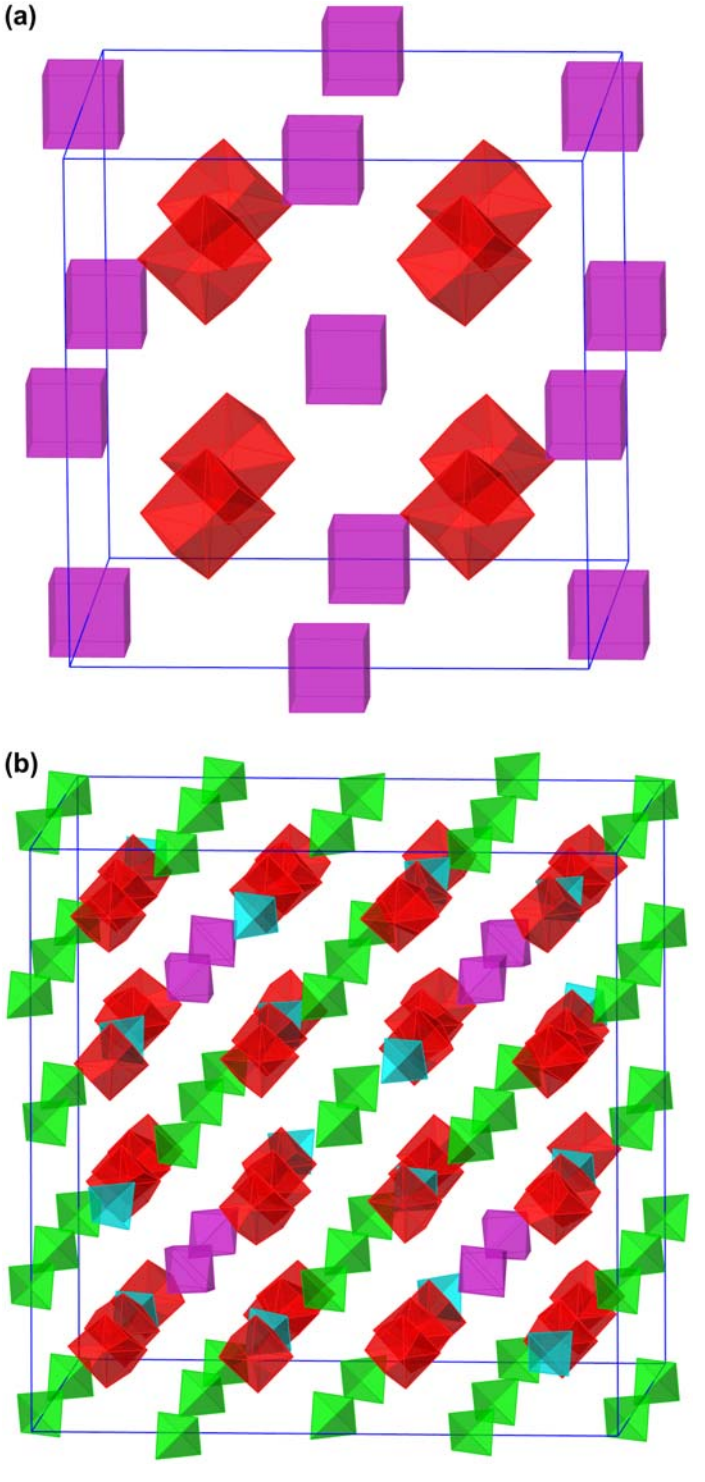

Figure 4. Arrangement of all BF_4^- anions in the unit cell of $[Co(NH_3)_6](BF_4)_3$ in phase I (a) and phase II (b).

bonds are equal to 1.970 and 1.966 Å. The N–Co–N angles in the deformed octahedron are between 89.71° and 90.29°. There are four types of BF_4^- differing in their orientational disorder in phase II. As described earlier, there are 12 anions in the unit cell in phase I. One (out of four) cubic anion and six (out of eight) adamantane anions retained in phase II remain orientationally disordered. The rest of the anions become ordered and differ only in the degree of distortion in phase II (see table 3). The anionic packing in phase II is illustrated in figure 4(b). The type of orientational disorder of the anions of this compound in phase II is exactly the same as that of $[Co(NH_3)_6](ClO_4)_3$ in phase II.

To understand the mechanism of the phase transition at T_{C1}, we analyze the closest neighborhood of the anions whose rotational dynamics has changed in phase II. Figure 5 shows the nearest surroundings of two types of anions, marked as B1 and B3, corresponding to the disordered cubic anion and the anion of adamantane geometry whose orientation is ordered below T_{C1}, respectively. For better clarity, all BF_4^- anions are depicted only by the B atoms. The B1 cubic anion is located inside the octahedral cavity formed by six deformed $Co(NH_3)_6^{3+}$ cations. The shortest N–B1 distance from these six cations is the same for all and is 3.618 Å. This cationic cavity is still sufficiently large for the anion to be disordered. The B1 cubic anion is also surrounded by eight anions, six of which are disordered with all the B1–B4 distances equal to 4.852 Å, while the remaining two are ordered and are located on the diagonal of the cubic cavity with the B1–B3 distances smaller than or equal to 4.753 Å. However, this bond length difference is due to the NH···F(B3) hydrogen-bonding interactions occurring below T_{C1}, which do not cause ordering of the B1 anion.

As illustrated in figure 5, the ordered anion represented by B3 is located inside the tetrahedral cavity formed by four cations (three deformed and one regular) as well as four anions (three ordered and one disordered). This anion is not symmetrically located in the cationic cavity but is shifted toward the three deformed cations with the closest N–B3

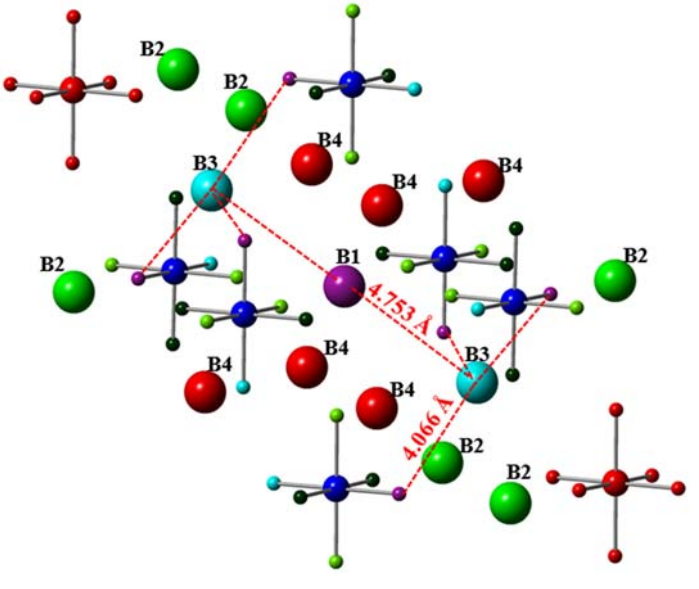

Figure 5. Nearest surroundings of B1 and B3 in phase II at 200 K, derived from disordered cubic BF_4^- (1) and ordered (from adamantane-type in phase I) BF_4^- (3).

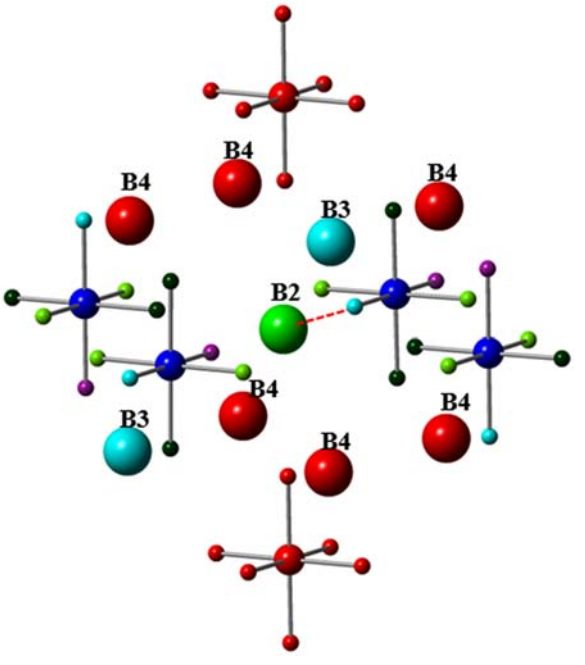

Figure 6. Nearest surroundings of B2 in phase II at 200 K, derived from ordered (from cubic-type in phase I) BF_4^- (2).

contacts being the same and equal to 4.066 Å. The distance from the fourth regular cation to the B3 anion is significantly longer with N–B3 equal to 4.108 Å. Thus, it is clear that the intermolecular interactions between the hosted anion and three deformed cations are the reason for ordering of the anion. The shortest B–B and N–B distances are shown in figure 5 with red dashed lines.

Figure 6 illustrates the nearest surroundings of the anion marked as B2 and includes every cubic anion whose orientation has been ordered below T_{C1}. There are six cations (four deformed and two regular) located octahedrally around the anion. In this case, the shortest B2–N distances are not the same. Five of them are in the range 3.623–3.647 Å and the sixth one, marked with a red dashed line in figure 6, is significantly shorter (B2–N2 of 3.591 Å). Therefore, the intermolecular N(2)H···FB(2) hydrogen-bonding interactions between the hosted anion and one of the six surrounding cations are the main reason for the ordering of this anion. The B2 anion is also located in the cubic cavity formed by eight surrounding anions (B3 and B4). Notably, this asymmetric anionic cavity directly affects the deformation of the host anion but not its ordering.

3.2.3. Crystal structure of phase III. The crystal structure of phase III was investigated at 100 K. The structure remains cubic with the lattice parameter $a = 22.2075(4)$ Å and $Z = 32$. There is a definite change of the Bravais lattice from body centered (I) to primitive (P). However, we were unable to solve the crystal structure because of various difficulties. The primitive cell gives many possibilities. The positions of BF_4^- could not be fixed because of the low mass. The crystal structure of phase III becomes more complex since

there are more different types of anions and cations existing in the crystal lattice in comparison with that of phase II, resulting in an increase in the number of parameters needed in the structural model. Nevertheless, we can safely say that some adamantane-type anions still remain disordered in phase III.

3.3. *Mechanism of phase transitions*

It is evident from our structural investigations that the orientational ordering of BF_4^- is strongly involved in phase transitions. Although we do not have any information about the crystal structure of phases IV and V, one can imagine that the disordered anions remaining in phase III may become completely ordered at $T=0$. If we simply assume that all the anions in phase I are disordered independently from each other between two distinct orientations and become completely ordered in phase V, then we arrive at the total entropy change of $3R \ln 2 = 17.3\,J\,K^{-1}\,mol^{-1}$. The experimental value of $15.4\,J\,K^{-1}\,mol^{-1}$ is slightly smaller than that expected. It can be justified by the fact that the anions are involved in a hydrogen-bonding network in the crystal and thus cannot be perfectly independent from each other. There must be some weak restriction, depending on the strength of the hydrogen bonds that prevents independent disordering in the high-temperature phases, which results in a slightly smaller entropy value. It is interesting to compare the entropy value obtained for this compound with that for $[Co(NH_3)_6](ClO_4)_3$ ($12.1\,J\,K^{-1}\,mol^{-1}$) [6]. The difference may indicate that the hydrogen-bond interactions in this compound are considerably weaker than those in $[Co(NH_3)_6](ClO_4)_3$, consistent with the conclusion from IR spectroscopy data for a series of divalent compounds [22].

3.4. *Energy required to reorientate an anion in phases II and III*

From the low-temperature tail of the heat capacity below the transition temperature, it is possible to estimate the energy required to rotate an ordered BF_4^- in the particular phase. Assuming that the number of BF_4^- anions in the wrong orientation n is very small in comparison with the total number of the ordered anions N, we have

$$\frac{n}{N} = \exp(s/k)\exp(-\varepsilon/kT) \tag{1}$$

where ε is the estimated energy and s is the corresponding entropy. The anomalous heat capacity ΔC is given by

$$\Delta C = \frac{1}{T^2}\frac{\varepsilon^2}{k}\exp(s/k)\exp(-\varepsilon/kT) \tag{2}$$

which is analogous to the case of vacancy formation [23]. When $\ln(T^2\Delta C)$ is plotted against $1/T$, as shown in figure 7, two straight lines are obtained for phases II and III. The slopes give $\varepsilon = 17.5$ and $10.3\,kJ\,mol^{-1}$, respectively. The magnitude of ε corresponds to the difference in the energy between the presence and absence of hydrogen bonding. Since the number of relevant hydrogen bonds in the formula unit involved in the transition from phase II to I is $(5/12)\times 3\times 4 = 5$, the corresponding energy of $3.5\,kJ\,mol^{-1}$ is required to break a hydrogen bond. This value is considerably smaller than that obtained for

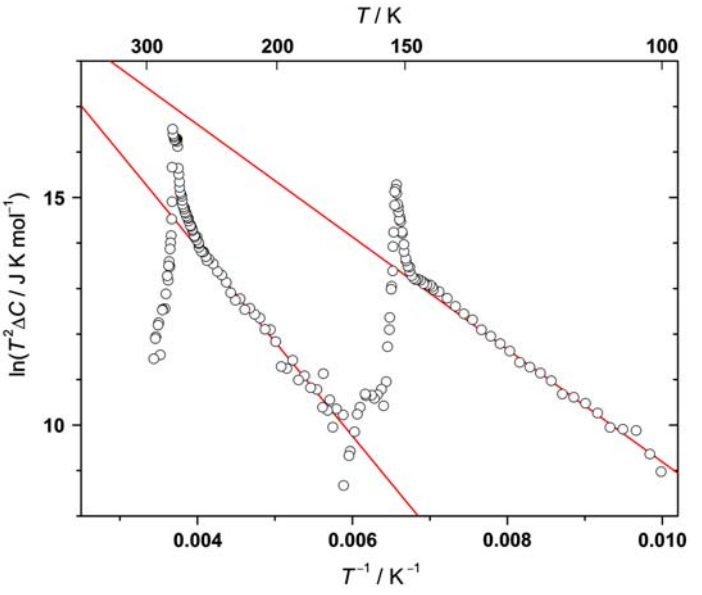

Figure 7. Evaluation of the energy required to reorient an ordered BF_4^- anion in the crystal lattice of phases II and III.

$[Co(NH_3)_6](ClO_4)_3$ in phase II (8 kJ mol^{-1}), indicating that the NH···F hydrogen-bonding interactions in this compound are considerably weaker than the NH···O interactions in the isostructural compound $[Co(NH_3)_6](ClO_4)_3$. Since the structure of phase III is unknown, the number of relevant hydrogen bonds involved in the transition from phase III to II is not available. However, we can safely say that the corresponding energy may be even smaller.

4. Conclusions

(1) $[Co(NH_3)_6](BF_4)_3$ exhibits four solid–solid phase transitions at $T_{C1} = 271.7$ K, $T_{C2} = 152.2$ K, $T_{C3} = 67.4$ K, and $T_{C4} = 48.9$ K. The former two transitions (II → I and III → II) are very sharp and distinct with the heat capacity tailing to the low-temperature side and are accompanied by large entropy changes of 8.4 and 6.5 J K^{-1} mol^{-1}, respectively. The latter two transitions (IV → III and V → IV) are accompanied by small entropy changes of 0.31 and 0.15 J K^{-1} mol^{-1}, respectively. They all are of the order–disorder type and connected with gradual ordering in the orientation of BF_4^-.

(2) In phase I, at 293 K, the compound crystallizes in the cubic space group $Fm\bar{3}m$ with $a = 11.2462(8)$ Å and $Z = 4$. One type of regular octahedral cation ($Co(NH_3)_6^{3+}$) and two types of tetrahedral BF_4^- ions varying in the orientational disorder are observed. In phase II, at 200 K, the compound crystallizes in the cubic space group $Ia\bar{3}$ with $a = 22.3460(4)$ Å and $Z = 32$. Two types of cations (one regular and one deformed) and four types of anions exist. Five out of 12 anions (in the unit cell) become

orientationally ordered in phase II. Weak but distinct NH···FB hydrogen-bonding interactions occurring in the network are responsible for ordering of these anions. The structure of phase III remains cubic.

(3) The energies required to reorient an ordered anion in the crystal lattice of phases II and III demonstrate that the NH···F hydrogen-bonding interactions in this compound are weaker than the NH···O interactions in an isostructural compound ($[Co(NH_3)_6](ClO_4)_3$). This may be the reason why the transition temperature T_{C1} is considerably lower in $[Co(NH_3)_6](BF_4)_3$ than in $[Co(NH_3)_6](ClO_4)_3$ (334.2 K) [6].

(4) In the revision process of our manuscript, we came across a paper on $[Mn(DMSO)_6](ClO_4)_2$ studied by NMR and Raman spectroscopy [24]. Although the system is rather different from ours, we share a common interest. Both materials show multiple phase transitions and their high-temperature phase is highly disordered.

Supplementay material

The heat capacity data obtained by adiabatic calorimetry are given in table S1 and the atomic coordinates and isotropic displacement parameters are listed in table S2. X-ray single-crystal diffraction data obtained at 293 K and 200 K are available as combined CIF file.

Acknowledgment

This study is Contribution No. 27 from the Research Center for Structural Thermodynamics.

References

[1] J. Hetmańczyk, Ł. Hetmańczyk, A. Migdał-Mikuli, E. Mikuli, I. Natkaniec. *J. Alloys Compd.*, **509**, 6545 (2011).
[2] A. Migdał-Mikuli, E. Mikuli, S. Wróbel, Ł. Hetmańczyk. *Z. Naturforsch. A*, **54**, 590 (1999).
[3] J.M. Janik, J.A. Janik, A. Migdał-Mikuli, E. Mikuli, K. Otnes. *Physica B*, **168**, 45 (1991).
[4] K. Parlinski. *Phys. Status Solidi B*, **98**, 487 (1980).
[5] S. Hodorowicz, M. Ciechanowicz-Rutkowska, J.M. Janik, J.A. Janik. *Phys. Status Solidi A*, **43**, 53 (1977).
[6] N. Górska, A. Inaba, Y. Hirao, E. Mikuli, K. Hołderna-Natkaniec. *RSC Adv.*, **2**, 4283 (2012).
[7] R.G.W. Wyckoff. *Cryst. Struct.*, Vol. 3, Wiley/Interscience, New York, NY (1965).
[8] E. Mikuli, N. Górska, S. Wróbel, J. Ściesiński, E. Ściesińska. *J. Mol. Struct.*, **692**, 231 (2004).
[9] E. Mikuli, N. Górska, S. Wróbel, J. Ściesiński, E. Ściesińska. *Z. Naturforsch. A*, **62**, 179 (2007).
[10] H.C. Stynes, J.A. Ibers. *Inorg. Chem.*, **10**, 2304 (1971).
[11] G.R. Murray, J.S. Waugh. *J. Chem. Phys.*, **29**, 207 (1958).
[12] J. Bjerrum, J.P. McReynolds, *Inorganic Syntheses*, Vol. 2, p. 218, McGraw-Hill Book, New York (1946).
[13] T. Matsuo, K. Kohno, A. Inaba, T. Mochida, A. Izuoka, T. Sugawara. *J. Chem. Phys.*, **108**, 9809 (1998).
[14] H. Suzuki, A. Inaba, J. Krawczyk, M. Massalska-Arodź. *J. Chem. Thermodyn.*, **40**, 1232 (2008).
[15] G.M. Sheldrick. *SHELX-97. Acta Crystallogr. A*, **64**, 112 (2008).
[16] M.C. Burla, R. Caliandro, M. Camalli, G.L. Cascarano, L. De Caro, C. Giacovazzo, G. Polidori, R. Spagna. *SIR2004. J. Appl. Crystallogr.*, **38**, 381 (2005).
[17] K. Wakita, *Yadokari-XG, Software for Crystal Structure Analyses* (2001); Release of Software (Yadokari-XG 2009) for Crystal Structure Analyses, C. Kabuto, S. Akine, T. Nemoto, E. Kwon. *J. Cryst. Soc. Jpn.*, **51**, 218 (2009).
[18] J. Hetmańczyk, A. Migdał-Mikuli, Ł. Hetmańczyk. *Ann. Pol. Chem. Soc.*, **358**, (2007).

[19] M. Rachwalska, J.M. Janik, J.A. Janik, G. Pytasz, T. Waluga. *Phys. Status Solidi A*, **30**, K81 (1975).
[20] A. Migdał-Mikuli, E. Mikuli, M. Rachwalska, S. Hodorowicz. *Phys. Status Solidi A*, **47**, 57 (1978).
[21] T. Grzybek, J.A. Janik, J. Mayer, G. Pytasz, M. Rachwalska, T. Waluga. *Phys. Status Solidi A*, **16**, K165 (1973).
[22] R. Eβmann. *J. Mol. Struct.*, **351**, 87 (1995).
[23] R.H. Beaumont, H. Chihara, J.A. Morrison. *Proc. Phys. Soc. (London)*, **78**, 1462 (1961).
[24] E. Szostak, A. Migdał-Mikuli, K. Hołderna-Natkaniec, R. Gwoździk-Bujakowski, A. Kaczor. *J. Coord. Chem.*, **65**, 2732 (2012).